Neuro-Oncology 15(9):1225–1235, 2013.
doi:10.1093/neuonc/not052
Advance Access publication May 2, 2013

Enhancing drug delivery for boron neutron capture therapy of brain tumors with focused ultrasound

Ryan D. Alkins, Peter M. Brodersen, Rana N. S. Sodhi, and Kullervo Hynynen

Department of Medical Biophysics, University of Toronto, Ontario, Canada (R.D.A., K.H.); Sunnybrook Research Institute, Sunnybrook Health Sciences Centre (R.D.A., K.H.), and Surface Interface Ontario, University of Toronto (P.M.B., R.N.S.S.), Toronto, Ontario, Canada

Background. Glioblastoma is a notoriously difficult tumor to treat because of its relative sanctuary in the brain and infiltrative behavior. Therapies need to penetrate the CNS but avoid collateral tissue injury. Boron neutron capture therapy (BNCT) is a treatment whereby a ^{10}B-containing drug preferentially accumulates in malignant cells and causes highly localized damage when exposed to epithermal neutron irradiation. Studies have suggested that ^{10}B-enriched L-4-boronophenylalanine-fructose (BPA-f) complex uptake can be improved by enhancing the permeability of the cerebrovasculature with osmotic agents. We investigated the use of MRI-guided focused ultrasound, in combination with injectable microbubbles, to noninvasively and focally augment the uptake of BPA-f.

Methods. With the use of a 9L gliosarcoma tumor model in Fisher 344 rats, the blood-brain and blood-tumor barriers were disrupted with pulsed ultrasound using a 558 kHz transducer and Definity microbubbles, and BPA-f (250 mg/kg) was delivered intravenously over 2 h. ^{10}B concentrations were estimated with imaging mass spectrometry and inductively coupled plasma atomic emission spectroscopy.

Results. The tumor to brain ratio of ^{10}B was 6.7 ± 0.5 with focused ultrasound and only 4.1 ± 0.4 in the control group ($P < .01$), corresponding to a mean tumor [^{10}B] of 123 ± 25 ppm and 85 ± 29 ppm, respectively. ^{10}B uptake in infiltrating clusters treated with ultrasound was 0.86 ± 0.10 times the main tumor concentration, compared with only 0.29 ± 0.08 in controls.

Conclusions. Ultrasound increases the accumulation of ^{10}B in the main tumor and infiltrating cells. These findings, in combination with the expanding clinical use of focused ultrasound, may offer improvements in BNCT and the treatment of glioblastoma.

Keywords: blood-brain barrier, brain-tumor barrier, imaging mass spectrometry, neutron capture, therapeutic ultrasound.

Glioblastoma is the most aggressive primary brain tumor and deserves attention on the basis of its universally poor prognosis. Treatment is hindered by the diffusely infiltrating nature of the tumor, and thus, glioblastoma may be regarded as a whole brain disease.[1] There is no cure, and until relatively recently, treatment consisted of surgical resection followed by radiation therapy, yielding a median survival of 9–12 months, with only 3%–5% of patients alive at 2 years.[2,3] The most significant advance in glioblastoma therapy in the previous 3 decades was the addition of temozolomide to radiotherapy and surgical resection, increasing the median survival to 14.6 months and 2-year survival to 27.2%.[4,5]

The dismal prognosis associated with glioblastoma is attributable not only to its aggressive and infiltrative behavior, but also to its location typically deep in the parenchyma of the brain. Surgical corridors and extent of resection are limited by the potential for further neurological injury. Photon-based radiation therapy is a mainstay of treatment but causes significant collateral injury to the brain that worsens over time.[6,7] Finally, the endothelial cells of the brain's microvasculature are interconnected by tight junctions, forming the blood-brain barrier (BBB) between the circulating blood and the interstitial fluid space of the brain.[8] The BBB tightly regulates the passage of molecules into the brain, limiting the accumulation of many therapeutic agents, particularly in infiltrating cells advancing beyond the tumor margin.[9] The blood-tumor barrier (BTB) is variably more permeable but remains a significant obstacle to therapy.[10]

Received May 14, 2012; accepted March 7, 2013.

Corresponding Author: Ryan Alkins, MD, Sunnybrook Research Institute, Sunnybrook Health Sciences Centre, 2075 Bayview Ave., Toronto, Ontario, Canada M4N 3M5 (ralkins@sri.utoronto.ca).

Particularly in the brain, therapies should spare healthy tissue as much as possible, but many of those that have selective activity against malignant cells are hindered by the cerebrovasculature. Boron neutron capture therapy (BNCT) restricts the effects of ionizing radiation to malignant cells by exploiting the high thermal neutron capture cross-section of ^{10}B but requires the preferential delivery of a ^{10}B-containing carrier molecule to the tumor. We investigated focused ultrasound in combination with ultrasound contrast agents to increase the uptake of ^{10}B in malignant cells by focally increasing the permeability of the BBB and BTB.

BNCT is a binary treatment whereby a compound containing ^{10}B is formulated, such that it is taken up preferentially by tumor cells after administration into the blood. The tumor and surrounding tissue are then irradiated with a thermal or epithermal neutron beam, wherein ^{10}B captures a neutron to form ^{11}B and then rapidly undergoes alpha decay (Equation 1). The high linear energy transfer radiation produced in this reaction by the recoiling alpha particle and lithium ion has a range of approximately 5–9.

$$^{10}\mathrm{B} + n_{\mathrm{th}} \rightarrow [^{11}\mathrm{B}] \rightarrow {}^{4}\mathrm{He}(\alpha) + {}^{7}\mathrm{Li} + 2.79\ \mathrm{MeV} \quad (1)$$

μm in tissue, or on the order of a single cell, and results is DNA damage that is irreparable and potentially lethal.[11] Only ^{10}B-containing cells, given a sufficient intracellular concentration, will be eradicated, and other cells will be relatively spared. Successful BNCT thus requires an adequate concentration of ^{10}B in target cells, estimated to be on the order of 20 μg/g and a high tumor-to-brain ratio of ^{10}B.[11,12] This high ratio is desirable as it increases the relative dose to the tumor, while minimizing the number of hydrogen, nitrogen, and boron capture reactions that occur in nontarget tissues.

One of the 2 most commonly studied ^{10}B delivery agents is L-4-boronophenylalanine (BPA), which is complexed with fructose (BPA-f) to increase its solubility.[13] As an amino acid analogue, it accumulates preferentially in malignant cells because of comparatively higher metabolism. Early clinical trials of BNCT for glioblastoma used 2-h intravenous infusions of BPA-f, at doses ranging from 100 to 400 mg/kg body weight.[12,14,15] In animal glioblastoma models, however, significant improvements have been obtained by dose escalation, prolonged infusions, intra-carotid injection, and pharmacological or osmotic BBB disruption (BBBD) before drug administration.[16–18] More recently, transient, focal BBBD has been demonstrated using focused ultrasound.[19] With the use of low-energy ultrasound bursts at sub-megahertz frequencies through the intact skull, in combination with timed intravenous injections of encapsulated perfluorocarbon microbubbles, the permeability of the cerebral microvasculature can be increased.[20,21] Although the underlying mechanisms are not fully understood, cavitation of microbubbles under the influence of ultrasound pulses appears to cause temporary mechanical disruption of the endothelial tight junctions and increased para- and transcellular passage of molecules from the blood into the brain.[22] Gadolinium-enhanced MR imaging is used to identify the regions of contrast extravasation and confirm BBBD.[20,21]

In a rodent model of glioblastoma, we postulated that increasing the vascular permeability in and around the tumor (BBB/BTB disruption, hereafter referred to as BBBD) with MR-guided focused ultrasound would result in an increased and more uniform uptake of intravenously administered BPA-f into the tumor.

Materials and Methods

BPA (98.4% purity, Interpharma Praha, Prague, Czech Republic) was prepared without the use of glass labware to avoid contamination from borosilicate glass.[23] The ^{10}B enrichment was confirmed by ToF-SIMS. The BPA-f complex was prepared as described previously in the literature.[13,24] It was refrigerated in a polypropylene vessel overnight and passed through a 0.22 μm filter before administration.

Tumor Implantation

All procedures were approved by the institutional animal care committee and conformed to the guidelines of the Canadian Council on Animal Care. General anesthesia was induced in male Fisher 344 rats weighing 250–300 g with isofluorane and maintained with a combination of ketamine (90 mg/kg), xylazine (10 mg/kg), and isofluorane. Tumors were implanted in the left frontal striatum with use of a stereotactic frame at a depth of 4 mm from the cortical surface. The 9L gliosarcoma cell line was selected because it has been extensively used in BNCT studies.[25] With the use of a 5-μL Hamilton syringe, 2.5×10^5 9L gliosarcoma cells were injected in 2 μL of media. Animals were imaged and treated 8–9 days after implantation, after the tumors had reached 1.5–2 mm in diameter.

Animal Preparation, Focused Ultrasound, and MRI Imaging

For ultrasound treatments, animals were anesthetized with ketamine and xylazine at the same dose previously detailed. A 22-gauge tail vein cannula was inserted and the head of the animal shaved and chemically depilated. Definity ultrasound contrast (Lantheus, North Billerica, MA) was prepared as directed and diluted 1:10 in normal saline. Animals were positioned supine and fixed in place with a bite bar and lower extremity restraints. The head was coupled to a single element concave ultrasound transducer (center frequency 558 kHz, $F = 0.8$, $R = 10$ cm) through a bath of degassed water. The free-field peak rarefaction pressure was measured to be 0.4 MPa. After MRI coregistration, a computer-controlled 3-axis positioning system allowed the focal spot of the transducer to be positioned at any location in the brain. All treatments began with baseline T2- and T1-weighted MR imaging, including a T1-weighted sequence with gadolinium contrast

(0.2 mL/kg; Omniscan, GE Healthcare, Milwaukee, WI), to identify the tumor. A single sonication was performed on each animal, each consisting of ultrasound bursts of 10 ms in length, repeated once every second (pulse repetition frequency of 1 Hz) for each corner of a 1.5 mm square in the axial plane (Fig. 1). The total treatment duration was 120 s. With the initiation of each sonication, animals were given a 0.02 mL/kg Definity bolus in the tail vein catheter, followed by a 0.5 mL saline flush. The same MR imaging sequences performed before treatment were then repeated after the sonication to confirm the extent and location of BBBD. Contrast enhancement (CE) on T1-weighted images was calculated as $CE = (I_{post} - I_{pre})/I_{pre}$, where I_{pre} and I_{post} are the pre- and postcontrast mean signal intensities of the tumor, each normalized by the intensity in the contralateral hemisphere. The CE was then used to characterize the increase in vascular permeability because of the sonication.

Treatment Groups

There was one tumor treatment group ($n = 3$) and one control tumor group ($n = 4$). All animals were delivered a BPA-f dose of 250 mg/kg body weight via tail vein catheter over a 2 h period and sacrificed 1 h after the conclusion of the infusion (3 h after the initiation of the treatment). In both groups, 25% of the total dose was delivered as an initial bolus, followed by a single sonication to induce BBBD. The remaining BPA-f was delivered over a 2-h infusion. The control group received only the 2-h infusion after the bolus. As an additional control, 2 animals ($n = 2$) without tumor implantation underwent BBBD with BPA-f infusion to evaluate the effect on normal brain, with the contralateral unsonicated hemisphere serving as a matched control.

Specimen Preparation

Animals were sacrificed by intravenous injection of euthanyl. Specimen preparation was similar to that described in the literature for ion imaging.[26,27] Animals were not perfused, because any ^{10}B present in the vasculature at the time of irradiation would contribute to the overall radiation dose delivered to the respective tissue. Brains were removed and flash-frozen in isopentane cooled in liquid nitrogen, then maintained at $-80^{\circ}C$ until the time of histological preparation. Ten-micrometer thick coronal sections, at 250-μm levels, were cut using a cryostat (Leica Microsystems GmbH, Wetzlar, Germany) with the chamber held at $-20^{\circ}C$ and immediately mounted on 50 mm N-type semiconducting silicon wafers (Wafer World, West Palm Beach, FL) maintained at the same temperature. The silicon-mounted sections were then lyophilized for 24 h and stored at room temperature in hermetically sealed containers with Drierite

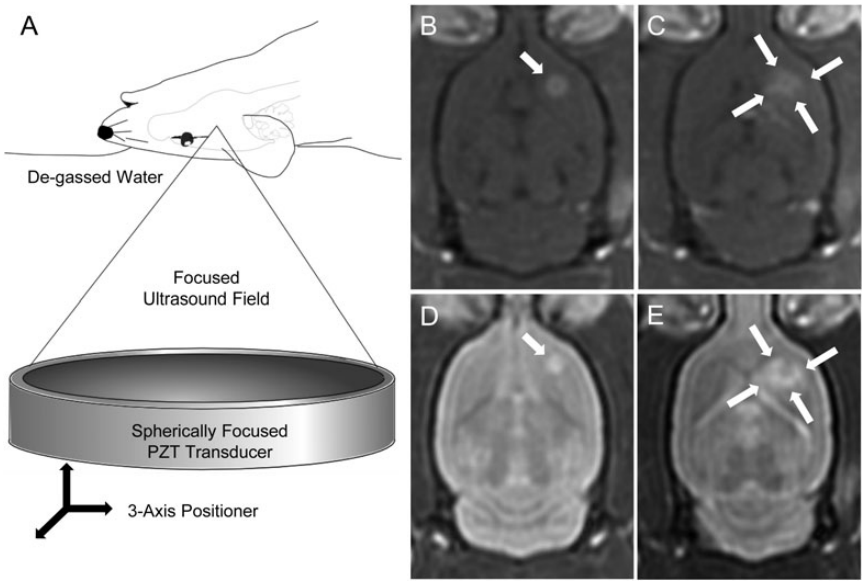

Fig. 1. Representative images of the rodent brain before and after BBBD with focused ultrasound. A schematic diagram is shown in (A) with the positioning of the animal relative to the ultrasound transducer. The 3-axis positioning system allows the transducer to be positioned so that the focal spot can be targeted anywhere in the brain. (B and C) Omniscan™ enhanced pre- and post-BBBD T1-weighted MR images, respectively. (D and E) Corresponding T2-weighted MR images. The tumor is indicated by the single arrow in panels B and D before BBBD. The 4 sonication foci (arrows) can be identified in C and E encircling the tumor after BBBD. The square pattern is slightly distorted as a result of transmission through the skull. The increase signal on the T2-weighted images corresponds to edema induced by the disruption of the vasculature. There also appears to be some BBBD toward the midline, resulting from the postero-medial focus, which has resulted in contrast enhancement periventricularly in the left frontal lobe, in the anterior commissure, and in the anterior portion of the left thalamus. This is attributable to the 3 mm pressure full-width half-maximum (FWHM) lateral beam width, which combined with the skull distortion, would overlap these structures.

(W.A. Hammond Drierite Co., Xenia, OH) until analysis by ToF-SIMS. An adjacent frozen section at each level was mounted on a glass slide and stained with hematoxylin and eosin (H&E) for light microscopy.

Imaging Mass Spectrometry

Mass spectrometry was performed with a ToF–SIMS IV time-of-flight mass spectrometer (Ion-Tof GmbH, Munster, Germany), taking measurements at the tumor-brain interface, where both the main tumor (MT), islands of infiltrating tumor (IT), and normal brain could be analyzed. Samples were presputtered for 60 s with oxygen (36 nA) over a 400 × 400 μm area centered on the region of interest. Positive secondary ions were analyzed within 200 × 200 μm regions (128 × 128 pixels, 1 shot per pixel, 550 scans, 100 μs cycle time) in imaging mode with a Bi_1^+ liquid metal ion analysis gun (200 ns pulse) and noninterlaced oxygen sputtering (0.2 s sputter, 0.1 s pause). Imaging parameters were kept constant for all measurements. Regions for analysis were identified using a combination of optical imaging of cryosections and the corresponding H&E-stained slides. On average, 9 measurements were performed on 2–3 separate levels for each animal. To account for differences in secondary ion intensities between samples, the secondary ion intensity of ^{10}B was normalized by the intensity of ^{12}C, because the latter is a relatively uniform matrix element.[26] This same normalization was used for all other elements investigated. For the analysis of the IT regions, because they were not present in all sections and a particular island of cells was typically only visible in a single level, 2–3 IT regions were selected for each animal and the mean-normalized ^{10}B intensity was compared with that of the MT in the same section. The mean IT:MT ratio of ^{10}B was then calculated for the BBBD and control groups.

Inductively Coupled Plasma Atomic Optical Emission Spectroscopy (ICP-AES) and Semi-Quantification of ToF-SIMS Data

Boron concentrations were measured with a Perkin-Elmer Optima 7300 DV ICP-AES using the 249.7 nm line of boron. Whole blood samples were collected at the time of sacrifice, digested with trichloroacetic acid (Sigma Aldrich), and centrifuged, and the supernatant was analyzed for total boron concentration as described elsewhere.[28] To convert the secondary ion intensities obtained with ToF-SIMS to concentration values (ppm), 9L cell pellets were enriched with BPA-f, homogenized, and frozen. These were digested using a combination of concentrated double distilled nitric and hydrochloric acid stored in Teflon (Veritas, GFS Chemicals, Columbus, OH), and the concentration of total boron was measured.[26] Magnesium was also measured in these specimens with both ToF-SIMS and ICP-AES (285.2 nm line) to help confirm uniform tissue processing between samples. The boron concentrations in the samples were then calculated using a relative sensitivity, factor as shown in Equation 2, where I_B, I_C, and $[B]$ are the secondary ion intensities of

$$[B]_{\text{sample}} = \frac{I_{B\_\text{sample}}}{I_{C\_\text{sample}}} \frac{I_{C\_\text{control}}}{I_{B\_\text{control}}} [B]_{\text{control}} \qquad (2)$$

^{10}B and ^{12}C and the concentration of ^{10}B in ppm wet weight, respectively, for the sample of interest, and the control samples were digested and analyzed using ICP-AES.[26]

Statistical Analysis

GraphPad Prism 5 (GraphPad Software, San Diego, CA) was used for statistical analysis. ToF-SIMS spectrums were analyzed and Poisson corrected with SurfaceLab6 (Ion-Tof GmbH, Munster, Germany) before analysis with GraphPad. Ratios were calculated as the mean ± standard error of the individual tumor to brain boron ratios for each animal. Boron concentrations (mean ± standard deviation) were estimated from the mean secondary ion intensity for each of the ultrasound-treated tumor, control tumor, and normal brain with use of Equation 2 and the ICP-AEOS measurements of the doped cell pellets. Student's *t* test was used to compare the means ± standard deviation and means ± standard error of the mean from 2 groups.

Results

All animals tolerated the drug infusion and ultrasound treatment without complication and recovered from general anesthesia to their pretreatment condition before sacrifice. Figure 1 depicts representative T2-weighted and contrast-enhanced T1-weighted MR images before and after BBBD. The increase in contrast extravasation after treatment with ultrasound was relatively uniform; the mean contrast enhancement of the tumor region without BBBD was 12.5% ± 0.7%, and after BBBD, it was 46% ± 4% ($P < .01$). Although the BTB is permeable, these results demonstrate that it can be made more so with the combination of ultrasound and microbubbles. T2-weighted imaging shows an increase in edema after BBBD as a result of the increased capillary permeability (Fig. 1E). All animals received the same weight-based dose of BPA-f, and whole blood samples obtained from both sonicated and control animals, analyzed by ICP-AES, showed no statistically significant difference in total boron concentration at the time of sacrifice.

On thorough histological review of the brain, no tissue injury was identified as a result of the ultrasound exposure; specifically, there were no regions of red blood cell extravasation, vacuolation, or abnormal neurons (pyknotic or karyorrhexic). Light microscopic review of H&E sections was used to select regions of interest for ToF-SIMS analysis on the corresponding adjacent silicon wafer–mounted sections. The tumor was easily differentiated from the normal brain tissue with the use of optical imaging in the vacuum chamber of the

ToF-SIMS instrument (Fig. 2A). A ToF-SIMS method was developed for the measurement of boron in cryogenically prepared specimens, which increased the sensitivity to elemental boron by >40-fold, compared with the initial imaging parameters, using bismuth as a primary ion source without oxygen sputtering. To our knowledge, this is the first use of a time-of-flight SIMS instrument to measure boron in the brain relating to BNCT. Although the secondary ion signals due to sodium and potassium saturated the detector, which precluded accurate quantitative comparisons of these particular ions, the $^{39}K/^{23}Na$ ratio ranged from 2:1 to 5:1 and did not correlate with the ^{10}B distribution. These results suggest that the cryoprocessing of the samples was acceptable.[29] Imaging of sodium and potassium also helped delineate structural details of the tumor. As has been similarly reported in ^{23}Na MR imaging of human brain tumors, the secondary ion intensity of ^{23}Na was higher in the tumor than in the adjacent normal brain tissue.[30] Representative secondary ion images of $^{23}Na^+$, $^{39}K^+$, $^{12}C^+$, and $^{10}B^+$ are shown at the tumor-brain interface in Fig. 3. In the tumors, $^{10}B^+$ appeared to be distributed without any appreciable pattern relative to cellular structure. As reported in previous mass spectrometry studies of rodent tumors, a higher concentration of $^{25}Mg^+$ was detected in 9L tumors than in the surrounding brain, and served to further differentiate tumor from nontumor regions.[17]

Representative images of the normalized [^{10}B] in ultrasound-treated tumor, control tumor, peri-tumoral healthy brain, and contralateral brain and these respective concentrations overlaid on the sum of the remaining secondary ion signal are shown in Fig. 4. Measurements of ^{10}B near the core of the tumor were compared with measurements taken at the periphery. There was no statistically significant difference among these measurements, likely in part because of the lack of a necrotic core in these relatively small 9L tumors; therefore, the entire volume was relatively well vascularized. Measurements of ^{10}B in normal brain tissue were also compared with those in the untreated contralateral hemisphere (Fig. 4C and D). Again, there was no statistically significant difference found ($P = .98$), suggesting that ultrasound does not augment the baseline uptake of BPA-f by nonmalignant cells in the brain. This was confirmed by the control group without tumor implantation, in which we found no significant difference between the ^{10}B concentration in the sonicated region and the contralateral hemisphere (21.3 ± 8.7 versus 17.8 ± 3.9 ppm; $P = .39$) (Fig. 5).

The mean ratio of ^{10}B in the tumor to that in the adjacent brain was 6.7 ± 0.5 in the group that underwent BBBD and only 4.1 ± 0.4 in the control group ($P < .01$). The mean [^{10}B] in the BBBD tumors was 123 ± 25 ppm, compared with 85 ± 29 ppm in the control tumors and 21 ± 5 ppm in the normal brain (Table 1). The range of [^{10}B] and the standard deviations of both the normal brain and tumors having undergone BBBD are proportionally smaller, suggesting less variation in ^{10}B distribution both in and among animals. This variability was very striking in the secondary ion intensities measured with ToF-SIMS, but after conversion to concentrations using ICP-AES, the measurement uncertainty from the latter dominated the error term. The range in all groups is shown in Table 1 and varies considerably more in the control tumor group (51–117 ppm). Although the 9L gliosarcoma does not exactly duplicate the infiltrative pattern of glioblastoma in humans,[16] the normalized ^{10}B intensity from small infiltrating islands of cells (IT) adjacent to the main tumor mass (IT) was measured. The [^{10}B] in the IT, of which a representative image is shown in Fig. 3, was found to be a

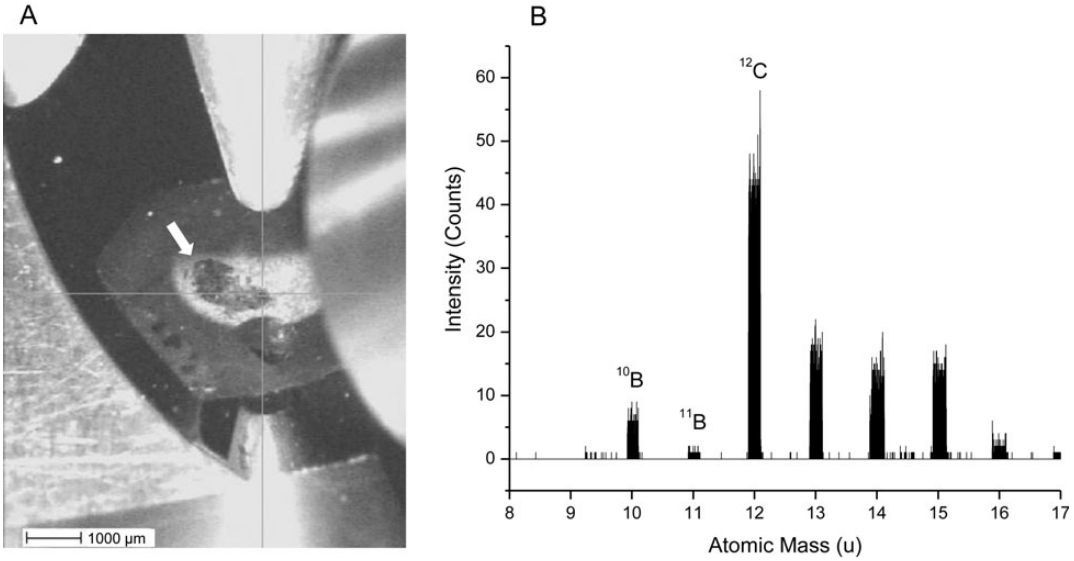

Fig. 2. Optical imaging in the vacuum chamber of the ToF-SIMS instrument was used to locate the tumor (indicated by the arrow) on the lyophilized specimens (A). After collection of the secondary ion spectra, the signal from $^{10}B^+$ was easily distinguishable because of the lack of interferences in that atomic mass range (B).

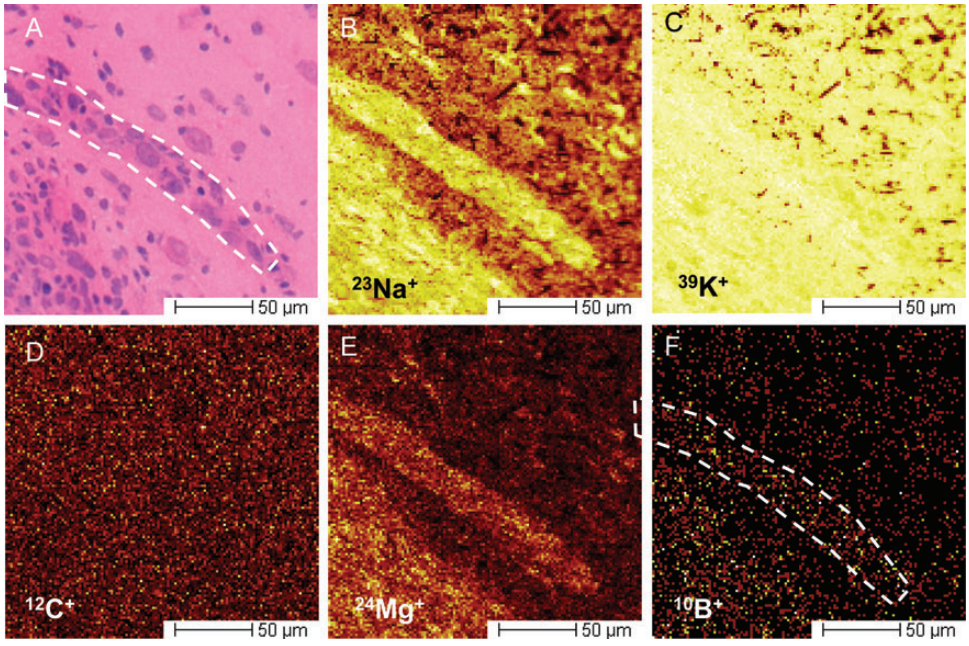

Fig. 3. Representative secondary ion images taken at the brain-tumor interface. The tumor can be identified in the lower left of each image, with an obliquely oriented island of tumor in the center. (A) Corresponding H&E-stained frozen section adjacent to that used for ToF-SIMS analysis. (B–F) were acquired simultaneously and are representative of the data sets collected. (D) The relatively uniform signal obtained from $^{12}C^+$ both in tumor and in normal brain tissue. For this reason, it is used as a reference element. Both $^{23}Na^+$ and $^{24}Mg^+$ can provide significant contrast between tumor and brain tissue (B and E), because the concentrations of both are higher in malignant cells. The boron content of the tumor is noticeably higher, compared with the brain (F).

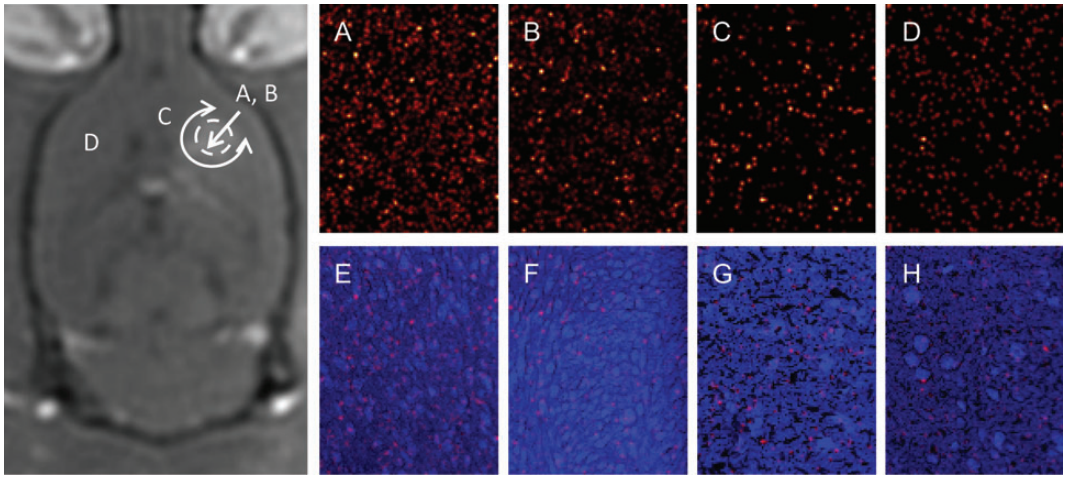

Fig. 4. ToF-SIMS imaging of a 150 × 200-μm region in the rat brain after infusion of BPA-f. The image on the left serves as a schematic of the relative locations in the brain from which the secondary ion signals were acquired. The adjacent 4 columns depict, from left to right, a tumor treated with ultrasound, a control tumor, the ipsilateral peritumoral normal brain, and the contralateral untreated brain. (A–D) The $^{10}B^+$ signal normalized by the $^{12}C^+$ signal. (E–H) The signal in A–D overlaid on the sum of the remaining secondary ion signal, where cellular detail can be appreciated. A, C, and D are all from the same animal. The quantitative results are presented in Table 1.

mean ($\pm$ standard error) of 0.86 ± 0.1 of the MT [^{10}B] in the BBBD group, compared with 0.29 ± 0.08 in the control group. This difference was found to be highly statistically significant ($P < .01$) and suggests that BBBD with focused ultrasound can improve the accumulation of ^{10}B in infiltrating tumor cells.

Discussion

Cure has been achieved with BNCT in rodent models of glioblastoma with use of prolonged infusion times, escalated doses (typically above 500 mg/kg), and intracarotid administration with osmotic BBBD. By comparison, in

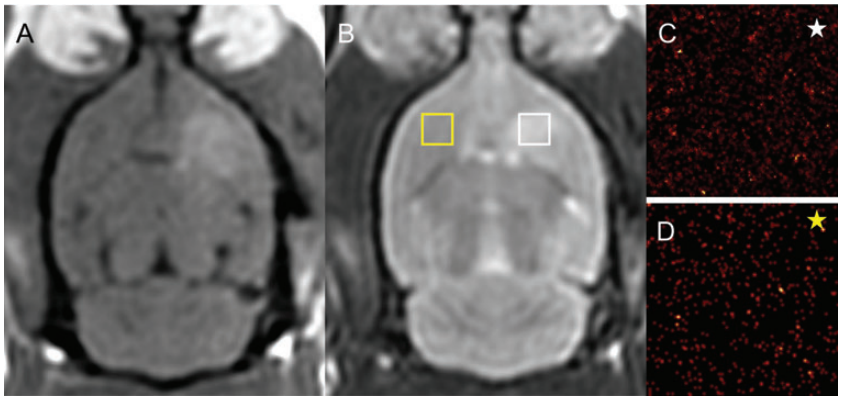

Fig. 5. MR imaging of BBBD without tumor implantation. Representative axial gadolinium-enhanced T1-weighted (A) and T2-weighted (B) MRI of BBBD without implanted tumors. The ^{10}B secondary ion signal obtained with ToF-SIMS from the sonicated (C) and unsonicated (D) frontal lobe is shown. The yellow and white boxes are not to scale but denote the approximate regions of analysis. The corresponding yellow and white stars denote the appropriate ToF-SIMS image. There was no statistically significant difference in the concentration in the normal brain tissue exposed to ultrasound ($P = .39$).

Table 1. Main tumor (MT) to brain and infiltrating tumor (IT) to brain ^{10}B ratios and tissue concentrations after BBBD with focused ultrasound and BPA-f infusion, compared with the control group receiving infusion alone

Group	MT:Brain ^{10}B Intensity[a]	[^{10}B] (ppm)[b]	[^{10}B] Range (ppm)	IT:MT ^{10}B Intensity[a]	IT [^{10}B] (ppm)[b]
BBB-D	6.7 ± 0.5**	123 ± 25	118–126	0.86 ± 0.10**	106 ± 25
Control	4.1 ± 0.4	85 ± 29	51–117	0.29 ± 0.08	25 ± 11
Normal Brain	–	21 ± 5	13–26	–	–

[a]Mean ± standard error.
[b]Mean ± standard deviation.
**$P < .01$.

humans, drug doses have been in the range of 100–400 mg/kg, according to the dose-escalation study conducted at Brookhaven National Laboratories.[15] BPA-f was found to precipitate in the urine at doses of >330 mg/kg (delivered over 2 h), raising the concern of renal injury at higher doses.[12,15] Furthermore, infusion times have also been relatively short (2 h), resulting in outcomes no different than those achieved with the current standard of care.[12] A recent exception was a Swedish phase II trial using a prolonged infusion time of 6 h and a dose of 900 mg/kg, to improve the efficacy of BNCT. Although higher blood levels were achieved at the time of treatment, compared with lower dose regimens, mean survival was 14.2 months, similar to that achieved with current standard therapy.[31] All patients had recurrent disease within 10 months after follow-up, and it was postulated that, as in prior studies, these early recurrences are secondary to heterogeneous drug uptake in the tumor, resulting in subtherapeutic radiation dosing in portions of the tumor.[17,31]

Preclinical studies have demonstrated increased accumulation of a number of therapeutic molecules, including BPA-f, in tumors of the brain after osmotic and pharmacological disruption of the BBB/BTB.[17,32,33] Local interstitial therapies have also been developed to circumvent these barriers, including drug-eluding wafers positioned in the resection cavity and catheter-based convection-enhanced delivery of targeted toxins and chemotherapeutic agents.[32–36] More recently, focused ultrasound has been shown to facilitate the entry of a number of therapeutic agents into the brain, focally and without significant adverse effects.[37–40] Although intra-arterial (IA) chemotherapy in combination with osmotic BBBD has had promising results in early clinical trials, Barth et al. reported that 10% of animals undergoing BBBD with IA mannitol died of cerebral edema.[41] The occurrence of massive cerebral edema with focused ultrasound is far less likely, because it can be restricted to the tumor and surrounding brain, rather than encompass the entire hemisphere. Furthermore, realizing intracarotid drug administration in humans requires cannulation of the internal carotid artery via endovascular techniques, which is not without risk. Compared with IA administration and interstitial therapies, the main advantages of ultrasound as an alternative for BBBD are its noninvasiveness and a more controlled and focal disruption of the cerebrovasculature. The latter may serve not only to reduce the risk of massive cerebral edema, but also to reduce the accumulation of BPA-f in healthy tissues and, thus, spare radiation exposure during BNCT and, particularly, with more neurotoxic chemotherapeutic agents, to reduce neurological adverse effects.

With ongoing advancements in the field of focused ultrasound and improved ultrasound contrast agents, safe

and reproducible BBBD is achievable. Preclinical studies in rodents have progressed to the investigation of BBBD in larger mammals, and BBBD has now been performed safely in large mammals and nonhuman primates, even through the intact skull.[42,43] The preliminary safety of transcranial therapeutic ultrasound in humans has been demonstrated, with the successful treatment of >30 patients for chronic pain and tremor with the use of similar techniques and treatment infrastructure.[44,45]

In the present study, we showed that using a relatively low dose of BPA-f, administered intravenously and delivered in combination with BBBD performed noninvasively with transcranial focused ultrasound, therapeutic tumor levels of ^{10}B can be achieved not only in the main tumor but also in infiltrating clusters of cells, without increasing the accumulation in healthy brain tissue (Table 1). These measurements were taken at 1 h after the termination of the BPA-f infusion, which we believe would reflect the concentrations at the time of treatment, allowing for patient transfer from the MRI environment to one suitable for neutron irradiation. Our results compare rather favorably to BPA-f distribution studies in the literature, and although we did not perform survival studies, we anticipate that similar gains in survival would be achieved. Smith et al. reported their findings in 9L-bearing Fisher 344 rats with use of 250 mg/kg body weight BPA-f over 2-, 3-, and 6-h intravenous infusions. The ^{10}B concentrations after a 2-h infusion, measured with a dynamic SIMS technique, were 83 $\pm$ 23 ppm in tumor and 20 $\pm$ 8 ppm in normal brain, comparing very closely with our control group (85 $\pm$ 29 ppm and 21 $\pm$ 5 ppm, tumor and brain respectively) (Table 1).[17] Only after a 6-h infusion did the tumor concentration reach 90 ppm, with less variability, compared with the shorter infusion time and a tumor to brain ratio of 5.0; however, the ratio and concentration are still slightly lower than that achieved with ultrasound-mediated BBBD after a 2-h infusion.[17]

We were not able to detect any change in the [^{10}B] in the normal brain tissue, owing to BBBD. This was thoroughly examined by comparing the peritumoral sonicated region with the contralateral hemisphere (Fig. 4) and sonicated normal brain with the unsonicated contralateral hemisphere in animals without tumors after BPA-f infusion (Fig. 5). These findings are supported by those of Smith et al.[17] and Barth et al.,[41] neither of whom detected a statistically significant difference between the ipsilateral and contralateral [^{10}B] with osmotic BBBD even with intracarotid administration. This is likely to have been attributable to the constant metabolic demand of the normal brain tissue; thus, increased bioavailability due to a more permeable BBB alone does not increase the uptake of amino acids (of which BPA is an analogue) into the cell by the L-amino acid transporter-1.[46] In brief, the normal brain appears to be adequately supplied through the intact BBB and, therefore, does not change its demand by an increased interstitial availability, particular when the intracellular concentrations are governed by active transport rather than diffusion alone. The interstitial concentration then begins to decrease immediately after the termination of the infusion,[28] as does the concentration in blood, because in the present study, the blood concentration was 15–20 ppm at 1 h after infusion. Measurements from human glioblastoma have found that the normal brain concentrations at similar time points were equal to or less than the blood concentrations, which is consistent with our findings within measurement error.[47] There is however some suggestion that reducing the peritumoral edema pharmacologically with dexamethasone can reduce the uptake of BPA-f in peritumoral brain, compared with the contralateral hemisphere, but this resulted in only a 14% difference,[48] a change that is likely to be too small to detect with the present technique.

Because many resections of glioblastoma are subtotal, the uptake of BPA-f into the main tumor mass is still of considerable importance. However, there is justifiable concern that infiltrating cells will not accumulate BPA-f to the same extent as the main tumor, where the BTB is more permeable than the BBB. We evaluated the [^{10}B] in small infiltrating clusters of tumor cells separated from the main tumor mass and found that BBBD with ultrasound resulted in a significantly improved [^{10}B], compared with infusion alone. In the BBBD group, the IT [^{10}B] was >80% of the MT concentration, and in the control group, it was only ~30% ($P < .01$). This latter result in the control group is comparable to results previously reported in the literature for a 2-h infusion of BPA-f.[17] The improved BPA-f uptake in infiltrating cells after BBBD with ultrasound is an important finding, because these cells are the most likely source of residual tumor after resection and are likely to be the cause of most eventual recurrences.

Another important finding is that the [^{10}B] in the tumors treated with focused ultrasound were more uniform than those in the control group, as evidenced by the wider range of measured concentrations and greater standard deviation of the concentrations in the latter (Table 1). This is perhaps not unexpected, because the increased capillary permeability of the tumor vessels is unlikely to be uniform throughout the tumor; this is attributabe to a variety of vascular phenotypes (some deficient in tight junction proteins)[49] and the influence of soluble factors (causing opening of normal tight junctions).[50] The combination of microbubbles and ultrasound, on the other hand, should cause a similar effect in the tumor and peritumoral vasculature, because they are wholly encompassed in the sonicated volume. The exact mechanisms through which cavitation disrupts the BBB are unknown, but they ultimately result in alterations in tight-junctional proteins and increased paracellular and transcellular permeability.[22] Although at higher sonication pressures, bubbles may collapse, generating fluid jets or shock waves,[51–53] at the pressures used in the present study, we expect that stable cavitation is the dominant mechanism, whereby BBBD is likely to be achieved via direct mechanical effects or microstreaming due to the oscillating microbubbles.[22,52] Regardless of the mechanism, this improved uniformity is an important finding, because there is no satisfactory in vivo assessment of the tumor boron concentration before neutron irradiation; thus, a more uniform BPA-f uptake would allow more reliable use of weight-based dosing or of a surrogate measurement (eg, blood-boron levels) and

lead to fewer patients being undertreated with BNCT. As previously mentioned, it has been theorized that this heterogeneous boron uptake with BPA-f infusions alone in human tumors may be responsible for the disappointing results in clinical trials.[17]

The present study is not without limitations. We have not conducted survival experiments, because we do not have access to a neutron source at our institution. However, the survival benefit of increased BPA-f accumulation in the 9L gliosarcoma and other rodent brain tumor models has been well studied.[16–18,25,41] We would expect similar improvements in survival when these improvements in BPA-f uptake are realized with ultrasound. Furthermore, there is recent evidence that ultrasound and microbubbles enhance the effect of radiation on endothelial cells;[54] thus, in theory, there could be a synergistic tumoricidal effect of BNCT and ultrasound-mediated BBBD. For acute studies such as this, the 9L gliosarcoma cell line is acceptable, but had we done survival studies, it would not have been a suitable choice. In addition, this cell line does not exactly mimic the infiltrative nature of glioblastoma in humans as previously discussed. Another limitation is the small blood volume in rodents, compared with humans; thus, the number of sonications was limited by the risk of volume overload. Optimization of the BPA-f infusion protocol used in conjunction with focused ultrasound could potentially be improved further in humans than in rodents. Drug penetration through the BBB/BTB with ultrasound was found to be most effective when BPA-f was in the circulation at the time of the sonication. However, uptake of BPA-f into cells is not only a function of the concentration to which they are exposed, but also to the duration of the exposure. As a result, a bolus was delivered before BBBD and then an infusion continued for 2 h afterward, knowing that the BBB remains open for ~6 h.[19] In theory, additional sonications could be performed during the infusion, which might serve to further augment the accumulation of BPA-f; however, in the present rodent model, the added fluid volume required would be injurious. A longer infusion time could potentially improve the accumulation of ^{10}B in infiltrating cells in the sonicated region.

Translating this treatment technology into humans requires careful consideration. A more sophisticated ultrasound setup than the one described here is required, because aberrations due to human skull cannot be neglected as they are in rodents. In humans, the skull is much thicker, but also heterogeneous, necessitating large phased arrays to maintain a tight focus.[55] Fortunately, there exists a commercial transcranial system manufactured by InSightec (Tirat-Carmel, Israel), which fits many of the requirements for BBBD to succeed in humans and has previously been used for transcranial applications in phase I human trials.[44,45] To improve transmission through bone, the system is available in a lower frequency (220 kHz) than the one used in the present study. This system is used in conjunction with MR-guidance to assess the degree of BBBD as we have done. Although some preclinical systems now use acoustic emissions to monitor BBBD,[56] this is not yet available in a clinical system although would likely serve to improve the safety of the treatment. A facility attempting to deliver this treatment would require an MRI suite accompanied with a hemispherical phased-array ultrasound system and a nearby neutron source; these requirements would limit this therapy to only a handful of sites in the world at present.

In summary, BNCT in humans requires further optimization to yield any benefit over conventional therapy. We have shown that BBBD with MR-guided focused ultrasound in combination with intravenous microbubbles safely augments BPA-f tumor uptake, compared with infusion alone. Increases the tumor to brain ^{10}B ratio not only for the main tumor, but also for infiltrating cells, with ^{10}B concentrations that compare very favorably with published results in the literature using higher doses and longer infusion. The narrower range of tumor ^{10}B concentrations in the tumors undergoing BBBD with ultrasound, in combination with higher accumulation of ^{10}B in infiltrating cells along the tumor-brain interface, may substantially reduce under-treatment with BNCT. As with BPA-f studies achieving a similar [^{10}B] in tumors, we would expect a similar improvement in survival and with expanding clinical investigations of therapeutic ultrasound, translation of these results to the clinical domain may soon be possible.

Acknowledgments

We thank Shawna Rideout-Gros and Alex Garces, for their assistance with the care of the animals; Milan Ganguly, for his expertise with histological preparation; Dr. Alison Burgess, for her help with the 9L cell culture; and Meaghan O'Reilly and Dr. Adam Waspe, for their technical assistance with the ultrasound system.

Conflict of interest statement. None declared.

Funding

This work was supported by the National Institutes of Health (R01EB003268) and the Canada Research Chair Program.

References

1. Halperin EC, Burger PC, Bullard DE. The fallacy of the localized supratentorial malignant glioma. *Int J Radiat Oncol Biol Phys*. 1988;15:505–509.
2. Ohgaki H, Dessen P, Jourde B, et al. Genetic pathways to glioblastoma: a population-based study. *Cancer Res*. 2004;64:6892–6899.
3. Adamson C, Kanu OO, Mehta AI, et al. Glioblastoma multiforme: a review of where we have been and where we are going. *Expert Opin Investig Drugs*. 2009;18:1061–1083.

4. Stupp R, Mason WP, van den Bent MJ, et al.; for the European organisation for research and treatment of cancer brain tumour and radiation oncology groups; National cancer institute of Canada clinical trials group. Radiotherapy plus concomitant and adjuvant temozolomide for glioblastoma. *N Engl J Med*. 2005;352:987–996.
5. Stupp R, Hegi ME, Mason WP, et al.; for the European organisation for research and treatment of cancer brain tumour and radiation oncology groups; National cancer institute of Canada clinical trials group. Effects of radiotherapy with concomitant and adjuvant temozolomide versus radiotherapy alone on survival in glioblastoma in a randomised phase III study: 5-year analysis of the EORTC-NCIC trial. *Lancet Oncol*. 2009;10:459–466.
6. Szerlip N, Rutter C, Ram N, et al. Factors impacting volumetric white matter changes following whole brain radiation therapy. *J Neurooncol*. 2011;103:111–119.
7. Crossen JR, Garwood A, Glatstein E, Neuwelt EA. Neurobehavioral sequelae of cranial irradiation in adults: a review of radiation induced encephalopathy. *J Clin Oncol*. 1994;12:627–642.
8. Abbott NJ, Rönnbäck L, Hansson E. Astrocyte-endothelial interactions at the blood-brain barrier. *Nat Rev Neurosci*. 2006;7:41–53.
9. Muldoon LL, Soussain C, Jahnke K, et al. Chemotherapy delivery issues in central nervous system malignancy: a reality check. *J Clin Oncol*. 2007;25:2295–2305.
10. Lockman PR, Mittapalli RK, Taskar KS, et al. Heterogeneous blood–tumor barrier permeability determines drug efficacy in experimental brain metastases of breast cancer. *Clin Cancer Res*. 2010;16:5664–5678.
11. Coderre JA, Morris GM. The radiation biology of boron neutron capture therapy. *Radiat Res*. 1999;151:1–18.
12. Barth RF, Coderre JA, Vicente MGH, Blue TE. Boron neutron capture therapy of cancer: current status and future prospects. *Clin Cancer Res*. 2005;11:3987–4002.
13. Yoshino K, Suzuki A, Mori Y, et al. Improvement of solubility of p-boronophenylalanine by complex formation with monosaccharides. *Strahlenther Onkol*. 1989;165:127–129.
14. Skold K, Gorlia T, Pellettieri L, Giusti V, H-Stenstam B, Hopewell JW. Boron neutron capture therapy for newly diagnosed glioblastoma multiforme: an assessment of clinical potential. *Br J Radiol*. 2010;83:596–603.
15. Diaz AZ. Assessment of the results from the phase I/II boron neutron capture therapy trials at the Brookhaven National Laboratory from a clinician's point of view. *J Neurooncol*. 2003;62:101–109.
16. Barth RF, Yang W, Coderre JA. Rat brain tumor models to assess the efficacy of boron neutron capture therapy: a critical evaluation. *J Neurooncol*. 2003;62:61–74.
17. Smith DR, Chandra S, Barth RF, Yang W, Joel DD, Coderre JA. Quantitative imaging and microlocalization of boron-10 in brain tumors and infiltrating tumor cells by SIMS ion microscopy: relevance to neutron capture therapy. *Cancer Res*. 2001;61:8179–8187.
18. Joel DD, Coderre JA, Micca PL, Nawrocky MM. Effect of dose and infusion time on the delivery of p-boronophenylalanine for neutron capture therapy. *J Neurooncol*. 1999;41:213–221.
19. Hynynen K, McDannold N, Vykhodtseva N, Jolesz FA. Noninvasive MR imaging-guided focal opening of the blood–brain barrier in rabbits. *Radiology*. 2001;220:640–646.
20. Hynynen K, McDannold N, Sheikov NA, Jolesz FA, Vykhodtseva N. Local and reversible blood–brain barrier disruption by noninvasive focused ultrasound at frequencies suitable for trans-skull sonications. *NeuroImage*. 2005;24:12–20.
21. McDannold N, Vykhodtseva N, Hynynen K. Use of ultrasound pulses combined with Definity® for targeted blood-brain barrier disruption: a feasibility study. *Ultrasound Med Biol*. 2007;33:584–590.
22. Sheikov N, McDannold N, Vykhodtseva N, Jolesz F, Hynynen K. Cellular mechanisms of the blood-brain barrier opening induced by ultrasound in presence of microbubbles. *Ultrasound Med Biol*. 2004;30:979–989.
23. Green GH, Blincoe C, WeethBoron HJ. Boron contamination from borosilicate glass. *J Agric Food Chem*. 1976;24:1245–1246.
24. Shibata Y, Zamenhof RG, Busse P, Patel H. Quality control of BPA-f for Harvard-MIT BNCT Clinical Trial [abstract]. 11th World Congress on Neutron Capture Therapy. October 11–15, 2004; Boston, MA.
25. Barth RF. Rat brain tumor models in experimental neuro-oncology: the 9L, C6, T9, F98, RG2 (D74), RT-2 and CNS-1 Gliomas. *J Neurooncol*. 1998;36:91–102.
26. Ausserer WA, Ling YC, Chandra S, Morrison GH. Quantitative imaging of boron, calcium, magnesium, potassium, and sodium distributions in cultured cells with ion microscopy. *Anal Chem*. 1989;61:2690–2695.
27. Benabdellah F, Seyer A, Quinton L, Touboul D, Brunelle A, Laprévote O. Mass spectrometry imaging of rat brain sections: nanomolar sensitivity with MALDI versus nanometer resolution by TOF–SIMS. *Anal Bioanal Chem*. 2010;396:151–162.
28. Laakso J, Kulvik M, Ruokonen I, et al. Atomic emission method for total boron in blood during neutron-capture therapy. *Clin Chem*. 2001;47:1796–1803.
29. Chandra S, Ausserer WA, Morrison GH. Evaluation of matrix effects in ion microscopic analysis of freeze-fractured, freeze-dried cultured cells. *J Microsc*. 1987;148:223–239.
30. Ouwerkerk R, Bleich KB, Gillen JS, Pomper MG, Bottomley PA. Tissue sodium concentration in human brain tumors as measured with ^{23}Na MR imaging. *Radiology*. 2003;227:529–537.
31. Henriksson R, Capala J, Michanek A, et al. Boron neutron capture therapy (BNCT) for glioblastoma multiforme: A phase II study evaluating a prolonged high-dose of boronophenylalanine (BPA). *Radiother Oncol*. 2008;88:183–191.
32. Kroll RA, Neuwelt EA. Outwitting the blood-brain barrier for therapeutic purposes: osmotic opening and other means. *Neurosurgery*. 1998;42:1083–1099.
33. Dean RL, Emerich DF, Hasler BP, Bartus RT. Cereport (RMP-7) increases carboplatin levels in brain tumors after pretreatment with dexamethasone. *Neuro Oncol*. 1999;1:268–274.
34. Sampson JH, Brady ML, Petry NA, et al. Intracerebral infusate distribution by convection-enhanced delivery in humans with malignant gliomas: descriptive effects of target anatomy and catheter positioning. *Neurosurgery*. 2007;60(suppl):ONS89–ONS98.
35. Rainov NG, Söling A. Clinical studies with targeted toxins in malignant glioma. *Rev Recent Clin Trials*. 2006;1:119–131.
36. Kunwar S, Chang S, Westphal M, et al. Phase III randomized trial of CED of IL13-PE38QQR vs Gliadel wafers for recurrent glioblastoma. *Neuro Oncol*. 2010;12:871–881.
37. Treat LH, McDannold N, Vykhodtseva N, Zhang Y, Tam K, Hynynen K. Targeted delivery of doxorubicin to the rat brain at therapeutic levels using MRI-guided focused ultrasound. *Int J Cancer*. 2007;121:901–907.
38. Escoffre JM, Piron J, Novell A, Bouakaz A. Doxorubicin delivery into tumor cells with ultrasound and microbubbles. *Mol Pharm*. 2011;8:799–806.
39. Liu HL, Hua MY, Chen PY, et al. Blood-brain barrier disruption with focused ultrasound enhances delivery of chemotherapeutic drugs for glioblastoma treatment. *Radiology*. 2010;255:415–425.

40. Kinoshita M, McDannold N, Jolesz FA, Hynynen K. Targeted delivery of antibodies through the blood–brain barrier by MRI-guided focused ultrasound. *Biochem Biophys Res Commun*. 2006;340:1085–1090.
41. Barth RF, Yang W, Rotaru JH, et al. Boron neutron capture therapy of brain tumors: enhanced survival following intracarotid injection of either sodium borocaptate or boronophenylalanine with or without blood-brain barrier disruption. *Cancer Res*. 1997;57:1129–1136.
42. McDannold N, Arvanitis CD, Vykhodtseva N, Livingstone MS. Temporary disruption of the blood-brain barrier by use of ultrasound and microbubbles: safety and efficacy evaluation in rhesus macaques. *Cancer Res*. 2012;72:3652–3663.
43. Xie F, Boska MD, Lof J. Effects of transcranial ultrasound and intravenous microbubbles on blood brain barrier permeability in a large animal model. *Ultrasound Med Biol*. 2008;34:2028–2034.
44. Jeanmonod D, Werner B, Morel A, et al. Transcranial magnetic resonance imaging-guided focused ultrasound: noninvasive central lateral thalamotomy for chronic neuropathic pain. *Neurosurg Focus*. 2012;32:E1.
45. Elias WJ, Huss D, Khaled M, et al. Results of a phase I study of MR-guided focused ultrasound thalamotomy for essential tremor [abstract]. American Association of Neurological Surgeons 80th Annual Scientific Meeting, April 14–18, 2012, Miami Beach, FL.
46. Detta A, Cruickshank GS. L-amino acid transporter-1 and boronophenylalanine-based boron neutron capture therapy of human brain tumors. *Cancer Res*. 2009;69:2126–2132.
47. Elowitz EH, Bergland RM, Coderre JA, Joel DD, Chadha M, Chanana AD. Biodistribution of p-boronophenylalanine in patients with glioblastoma multiforme for use in boron neutron capture therapy. *Neurosurgery*. 1998;42(3):463–468.
48. Morris GM, Micca PL, Coderre JA. The effect of dexamethasone on the uptake of p-boronophenylalanine in the rat brain and intracranial 9L glio-sarcoma. *Appl Radiat Isot*. 2004;61(5):917–921.
49. Rascher G, Fischmann A, Kröger S, Duffner F, Grote EH, Wolburg H. Extracellular matrix and the blood-brain barrier in glioblastoma multiforme: spatial segregation of tenascin and agrin. *Acta Neuropathol*. 2002;104:85–91.
50. Schneider SW, Ludwig T, Tatenhorst L, et al. Glioblastoma cells release factors that disrupt blood-brain barrier features. *Acta Neuropathologica*. 2004;107:272–276.
51. Ohl CD, Ikink R. Shock-Wave-Induced Jetting of Micron-Size Bubbles. *Phys Rev Lett*. 2003;90:214502.
52. Kodama T, Tatsuno M, Sugimoto S, Uenohara H, Yoshimoto T, Takayama K. Liquid jets, accelerated thrombolysis: a study for revascularization of cerebral embolism. *Ultrasound Med Biol*. 1999;25:977–983.
53. Dalecki D. Mechanical bioeffects of ultrasound. *Annu Rev Biomed Eng*. 2004;6:229–248.
54. Czarnota GJ, Karshafian R, Burns PN, et al. Tumor radiation response enhancement by acoustical stimulation of the vasculature. *Proc Natl Acad Sci U S A*. 2012;109:E2033–E2041.
55. Hynynen K, Jolesz FA. Demonstration of potential noninvasive ultrasound brain therapy through intact skull. *Ultrasound Med Biol*. 1998;24:275–283.
56. O'Reilly MA, Hynynen K. Blood-brain barrier: real-time feedback-controlled focused ultrasound disruption by using an acoustic emissions-based controller. *Radiology*. 2012;263:96–106.